

# Observation of a quarter of an electron charge at the $\nu = 5/2$ quantum Hall state

M. Dolev<sup>1</sup>, M. Heiblum<sup>1</sup>, V. Umansky<sup>1</sup>, Ady Stern<sup>1</sup> & D. Mahalu<sup>1</sup>

The fractional quantum Hall effect, where plateaus in the Hall resistance at values of  $h/\nu e^2$  coexist with zeros in the longitudinal resistance, results from electron correlations in two dimensions under a strong magnetic field. (Here  $h$  is Planck's constant,  $\nu$  the filling factor and  $e$  the electron charge.) Current flows along the sample edges and is carried by charged excitations (quasiparticles) whose charge is a fraction of the electron charge. Although earlier research concentrated on odd denominator fractional values of  $\nu$ , the observation of the even denominator  $\nu = 5/2$  state sparked much interest. This state is conjectured to be characterized by quasiparticles of charge  $e/4$ , whose statistics are 'non-abelian'—in other words, interchanging two quasiparticles may modify the state of the system into a different one, rather than just adding a phase as is the case for fermions or bosons. As such, these quasiparticles may be useful for the construction of a topological quantum computer. Here we report data on shot noise generated by partitioning edge currents in the  $\nu = 5/2$  state, consistent with the charge of the quasiparticle being  $e/4$ , and inconsistent with other possible values, such as  $e/2$  and  $e$ . Although this finding does not prove the non-abelian nature of the  $\nu = 5/2$  state, it is the first step towards a full understanding of these new fractional charges.

Theoretical predictions regarding the nature of the even denominator  $\nu = 5/2$  quantum Hall state rekindled strong interest in the fractional quantum Hall effect (FQHE)<sup>1–3</sup>. Primarily, this interest emanates from the unique properties of quasiparticles in this state, predicted by Moore and Read<sup>4,5</sup>: a fractional charge of a quarter of the electron charge ( $e/4$ ) and non-abelian quantum statistics. The quantum statistics are reflected in the evolution of the ground state wavefunction when two  $e/4$  quasiparticles are adiabatically interchanged. For conventional FQHE states, where the statistics are abelian, such an interchange merely multiplies the wavefunction by a phase. For non-abelian states, the presence of quasiparticles makes the ground state degenerate and an adiabatic interchange of two quasiparticles leads to a topological unitary transformation—where the topology of the path determines the transformation—that takes the system from one ground state to another. Unitary transformations that correspond to different interchanges do not generally commute with each other; hence the name non-abelian.

The topological nature of these transformations makes the  $\nu = 5/2$  state a test ground of the basic ideas of topological quantum computation, as it introduces remarkable immunity against decoherence and errors due to local uncontrollable perturbations<sup>6–8</sup>. Ideas proposed in these directions are based on interference experiments where inter-edge tunnelling of  $e/4$  quasiparticles takes place. For these experiments to succeed, two requirements should be satisfied: the first is that the  $\nu = 5/2$  state must be of the Moore–Read type, and the second is that the tunnelling quasiparticles must have charge  $e/4$ . These characteristics are predicted but not yet experimentally confirmed. The Moore–Read theory is based on a trial wavefunction inspired by considerations of conformal field theory<sup>4</sup>. It may be rederived<sup>9</sup> by considering weak Cooper pairing of composite fermions, which, under a magnetic field corresponding to the  $\nu = 5/2$  state, are fermions carrying an electron charge and two fictitious flux quanta. It is also supported by numerical exact diagonalization<sup>10</sup>. As for the second requirement, if electron or  $e/2$  quasiparticle tunnelling dominates over that of the  $e/4$  quasiparticles, inter-edge tunnelling

would not be a useful tool for examining the non-abelian statistics of the latter.

In this work we present shot noise measurements<sup>11,12</sup>, which result from partitioning of a stream of quasiparticles that tunnel between edge channels of a  $\nu = 5/2$  state. Measurements were performed on a patterned high-purity two-dimensional electron gas (2DEG) with a built-in constriction that allowed controlled tunnelling from one edge to another. From the dependence of the shot noise on the current, we deduced the charge of the quasiparticles, which was found to be consistent with charge  $e/4$ , and inconsistent with charge  $e/2$  or an electron charge  $e$ . In order to further validate the measurements, the charge of quasiparticles in other FQHE states in the vicinity of the  $\nu = 5/2$  state, such as at  $\nu = 5/3$ , 2,  $8/3$  and 3, was also measured by partitioning their current carrying states. Although these measurements do not directly probe non-abelian statistics, they do pave the way for such a measurement, which is likely to be based on interference effects<sup>13–16</sup>.

## The $5/2$ fractional quantum Hall state

The  $\nu = 5/2$  state is characterized by a zero longitudinal conductance and a Hall conductance plateau  $g_{5/2} = 5e^2/2h$ . At  $\nu = 5/2$ , the highly interacting electronic system can be mapped onto a system of weakly interacting, spin polarized, composite fermions at zero average magnetic field. The theory that predicts the  $\nu = 5/2$  state to be non-abelian starts with the Moore–Read wavefunction<sup>4</sup>. Within this theory, the composite fermions form a superconductor of Cooper pairs, with  $p_x + ip_y$  symmetry<sup>9</sup>, where the non-abelian quasiparticles are vortices, carrying half of a quantum flux,  $\phi_0/2 = h/2e$ . Because inserting these vortices costs a finite amount of energy (the Meissner effect in the condensate), the system is in an incompressible quantum Hall state with an energy gap for these excitations. With the flux carried by a vortex being  $h/2e$  and the uppermost Landau level half-filled, the charge that is associated with the quasiparticles was theoretically predicted<sup>4</sup> to be  $e^* = e/4$ . However, recent numerical

<sup>1</sup>Braun Center for Submicron Research, Department of Condensed Matter Physics, Weizmann Institute of Science, Rehovot 76100, Israel.

calculations raise the possibility that these quasiparticles may tend to form bound pairs of charge  $e/2$  (ref. 17). Only a small number of studies have thus far tested the predictions of Moore–Read theory<sup>4</sup>. The observed energy gap was measured to be significantly smaller than predicted<sup>18</sup>; the survival of the state in a small constriction was studied<sup>19</sup>; and the spin polarization of the state is thus far supported only by a numerical exact diagonalization method<sup>10</sup>. What makes measurements at the  $\nu = 5/2$  state rather scarce is the extreme fragility of that state. Only an extremely high-quality 2DEG and a rather low electron temperature support such states.

### Set-up and the basics of the measurements

The most important ingredient in our measurements is the GaAs–AlGaAs heterostructure that supports the 2DEG. The 2DEG has an electron density of  $\sim 3.2 \times 10^{11} \text{ cm}^{-2}$ , and a low-temperature mobility of  $30.5 \times 10^6 \text{ cm}^2 \text{ V}^{-1} \text{ s}^{-1}$ , measured in the dark (see Methods for more details). The Hall effect data, measured at 10 mK in a Hall bar 1 mm wide, revealed five significant fractions in the second Landau level,  $\nu = 11/5, 7/3, 5/2, 8/3$  and  $14/5$ , with a nearly zero longitudinal resistance at  $\nu = 5/2$  (Fig. 1a). These data indicate transport via edge channels with negligible current flowing in the bulk.

The samples were patterned in a shape of a Hall bar, with a single quantum point contact (QPC) in its centre and multiple ohmic contacts (Fig. 1b). The QPC partitioned the incoming current by bringing the forward propagating edge channel, with a chemical potential determined by the applied voltage  $V$ , into close proximity with the backward propagating edge channel returning from the grounded

contact (cold grounds<sup>20</sup>, see Methods for more details), hence inducing backscattering, partitioning and shot noise. A DC current  $I_{\text{imp}}$  was driven from the source contact (S), with the QPC partitioning it to the transmitted and backscattered currents. Shot noise, at 910 kHz, was amplified by a home-made preamplifier cooled to 4.2 K, with its output fed into a room temperature amplifier followed by a spectrum analyser (see Methods for more details). As long as the longitudinal resistance was zero, the resistance between terminals D and 2 was always the Hall resistance<sup>21</sup> (see Methods for more details).

We measured the two-terminal conductance and the current noise as a function of the source–drain voltage, at different partitioning values set by the QPC. Performing the noise measurements turned out to be challenging. A severe difficulty during the measurements was the instability and irreproducibility of the gates. Consequently, the desired partitioning by the QPC, which was determined by the filling factor within the QPC, was achieved by controlling the gate voltage (which controls the density within the QPC) simultaneously with tuning the magnetic field along a conductance Hall plateau in the bulk. This difficulty was compounded by the fact that the shot noise signal at the  $\nu = 5/2$  state is very weak. The spectral density of shot noise current fluctuations  $S^i$  is proportional to the effective charge  $e^*$  and to the impinging current in the partitioned edge channel. At  $\nu = 5/2$  the relevant partitioned current, which generates the noise, is only a small fraction of the total impinging current, depending on the next-lower channel within the QPC (for example, if the lower channel is  $\nu = 2$ , only  $1/5$  of the impinging current generates the noise). Furthermore, as our ‘cold preamplifier’ amplifies voltage fluctuations  $S^v$ , and  $S^v = S^i/(g_{5/2})^2$ , the large conductance at  $\nu = 5/2$  leads to a rather weak voltage signal.

### The analysis of shot noise

For the extraction of the quasiparticles’ charge, we use a rather simplified picture that was successful in analysing the shot noise of quasiparticles with charge  $e/3$  at  $\nu = 1/3$ ,  $e/5$  at  $\nu = 2/5$  and  $e/7$  at  $\nu = 3/7$  (refs 11, 20, 22). In this picture, we assume that in a conductance Hall plateau the current is being carried by quasiparticles in chiral edge channels with no bulk currents. When the bulk is in a certain conductance plateau and the QPC is wide open, the edge currents, which are noiseless (at zero temperature), traverse the QPC unaltered. As the QPC starts to close, the innermost forward propagating edge channel is coupled to the innermost backward propagating edge channel via tunnelling, leading to statistically independent backscattering events. Pinching the QPC further leads eventually to a full reflection of this partitioned edge channel with the conductance through the QPC reaching a lower conductance plateau.

When the conductance-dependent current through the QPC  $g(I_{\text{imp}})$  is in a transition between two plateaus, one corresponding to a lower lying state  $\nu_{i-1}$  (with conductance  $g_{i-1} = \nu_{i-1}e^2/h$ ) and another to the state above  $\nu_i$  (with conductance  $g_i = \nu_i e^2/h$ ), the current that impinges on the innermost channel is  $I_{\text{imp}}(i) = V\Delta g_i$  with  $\Delta g_i = g_i - g_{i-1}$ , where  $V$  is the applied DC voltage at the source. This current, which is in general smaller than the total impinging current  $I_{\text{imp}}$ , is being partitioned, hence generating shot noise. Similarly, the transmission of this channel’s current is defined as  $t_{\nu_i - \nu_{i-1}} = \frac{g(I_{\text{imp}}) - g_{i-1}}{\Delta g_i}$ . At zero temperature ( $T = 0$ ), the low frequency spectral density of the current fluctuations  $S^i(0)$  is related to the quasiparticle’s effective charge  $e^*$  through<sup>23,24</sup>:

$$S^i(0)_{T=0} = 2e^* V \Delta g_i t_{\nu_i - \nu_{i-1}} (1 - t_{\nu_i - \nu_{i-1}}) \quad (1)$$

At finite temperatures, the thermal contribution adds in and the shot noise is modified to the so-called ‘excess noise’<sup>25</sup>. The expression in equation (1) is then modified<sup>25</sup>:

$$S^i(0)_T = 2e^* V \Delta g_i t_{\nu_i - \nu_{i-1}} (1 - t_{\nu_i - \nu_{i-1}}) \left[ \coth\left(\frac{e^* V}{2k_B T}\right) - \frac{2k_B T}{e^* V} \right] + 4k_B T g \quad (2)$$

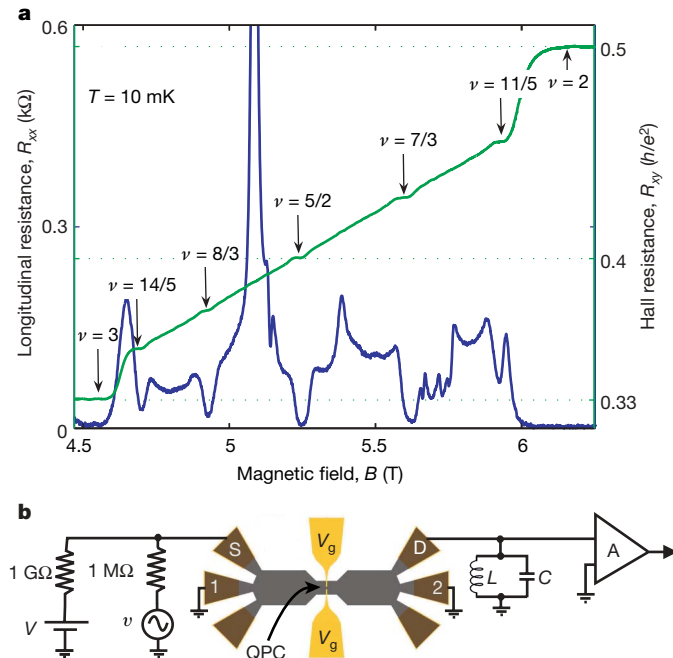


**Figure 1 | Quantum Hall effect in the second Landau level.** **a**, Hall resistance (green curve, right axis) and longitudinal resistance (blue curve, left axis) measured on an ungated Hall bar, 1 mm  $\times$  2.5 mm, with carrier density  $3.15 \times 10^{11} \text{ cm}^{-2}$  (determined at high magnetic field). The five main fractions,  $14/5, 8/3, 5/2, 7/3$  and  $11/5$  measured in a four-terminal configuration on the Hall bar, are highlighted. **b**, Diagram of the patterned sample and associated circuitry. Carrier density in this sample was  $3.27 \times 10^{11} \text{ cm}^{-2}$ . The two grounds, at 1 and 2, are ‘cold grounds’, cooling the electrons to  $\sim 10$  mK. DC current is driven to the sample through the source (S), provided by a DC voltage  $V$  and a large resistor in series. The AC voltage  $\nu$  is used to measure the conductance. Drain voltage (at D) is filtered with an LC resonant circuit, tuned to 910 kHz, and amplified by a preamplifier (A) cooled to 4.2 K, adjacent to the sample. The quantum point contact (QPC), controlled by  $V_g$ , is tuned for the desired transmission of the impinging current.

with  $k_B$  the Boltzmann constant. The assumption of statistical independence of the backscattered quasiparticles is expected to hold when  $t_{v_i-v_{i-1}}$  is close to zero (with rarely transmitted quasiparticles) or close to unity (with rarely reflected quasiparticles), but may be less reliable in intermediate values of  $t_{v_i-v_{i-1}}$ . Yet, previous works on Laughlin's quasiparticles have proved that if the nonlinear transmission is taken into account, then the prediction of the quasiparticles' charge from equations (1) and (2) agrees with the expected one. This might be attributed to the fact that equation (2) does have the correct limits at low and high temperatures, as well as the correct scale for the transition between the two.

### Identification of the structure of edge channels in the QPC

Deducing the charge from the measured shot noise (via equation (2)) requires a measurement of the relevant transmission  $t_{v_i-v_{i-1}}$  (defined above) and the corresponding impinging current  $I_{\text{imp}}(i)$ , which in turn requires the identification of the next-lower quantized Hall conductance  $g_{i-1}$  (the next to innermost edge channel) within the QPC. Our procedure for identifying the occupied channels in the QPC is demonstrated in Fig. 2. At low temperature, the transmission of the QPC depends strongly on the impinging DC current. This dependence does not generally agree with the prediction of the chiral Luttinger liquid (CLL) theory. As had been already observed before, in the integer and fractional quantum Hall regime<sup>19,26,27</sup>, under weak backscattering conditions of the  $i$ th state (the QPC is tuned to just below the  $i$ th plateau in the bulk, such that the  $i$ th edge channel is weakly backscattered), the transmission decreases with increasing DC current, exhibiting 'mound-like' behaviour. Alternatively, for strong backscattering conditions (the QPC is tuned to almost completely pinch off the  $i$ th state and the transmission is just above the lower lying ( $i-1$ )th plateau, such that the  $i$ th channel is almost fully backscattered), the transmission increases with DC current, exhibiting 'valley-like' behaviour. We attribute the 'mound-like' and 'valley-like' behaviours to a combination of several factors. Generally speaking, a larger applied voltage on the QPC barrier is expected to enhance the bare tunnelling probability for independent particles. 'Mound-like' behaviour appears in the limit of  $t_{v_i-v_{i-1}}$  close to unity, where tunnelling is between the forward and backward propagating channels. Then, tunnelling is responsible for the weak backscattering and thus applying larger voltage across the QPC increases backscattering and decreases the transmission. In contrast, 'valley-like' behaviour appears in the limit of  $t_{v_i-v_{i-1}}$  close to zero, where the high barrier is for forward tunnelling over the QPC; hence, tunnelling is responsible for the small transmission, which increases with the impinging current. The renormalization of the tunnelling rates predicted by the CLL presumably coexists with this mechanism. However, CLL alone cannot explain this reproducible 'mound-valley' behaviour, as it predicts enhancement of the tunnelling probability due to a decrease in the applied voltage. Altogether, as the QPC closes and the conductance crosses a quantized plateau, the transmission dependence on the impinging current switches from 'valley-like', to 'flat', and finally to 'mound-like' behaviour, offering us a way to identify the plateau that is being crossed.

We demonstrate this evolution in Fig. 2a, where we plot the dependence of the transmission on the total impinging DC current  $I_{\text{imp}}$  at bulk filling factor  $\nu_B = 3$ . The filling factor within the QPC,  $\nu_{\text{QPC}}$ , was varied either by the applied gate voltage  $V_g$  or by varying slightly the magnetic field within the bulk plateau of  $\nu_B = 3$ . One can follow the evolution from  $\nu_{\text{QPC}} = 3$  to  $\nu_{\text{QPC}} = 7/3$ , with a dependence on the impinging current as mentioned above. In Fig. 2b, we plot the dependence of the linear transmission (at zero DC current) on the filling factor in the QPC (the measurement was taken at two different gate voltages with a varying magnetic field at each gate voltage). Clear plateaus were observed within the QPC at  $\nu_{\text{QPC}} = 5/2$  and  $\nu_{\text{QPC}} = 7/3$ , and a weaker one at  $\nu_{\text{QPC}} = 8/3$ , in agreement with the values in Fig. 2a at which a transition was observed. Moreover,

at these plateaus no shot noise had been measured at a finite DC current.

The identification of a plateau that corresponds to a certain filling factor in the QPC under a certain gate voltage and magnetic field almost guarantees that this filling factor exists, as a lower lying state or as an outer edge channel, at higher values of QPC conductance. This is because at a less negative gate voltage (or a lower magnetic field) the QPC is more open, thus resembling the bulk and allowing the existence of incompressible regions within the QPC. However, the absence of such a plateau near an expected filling factor cannot rule out the existence of this lower lying state when the QPC is more open.

In some cases, at the lowest temperature of 10 mK the transmission of the QPC strongly depended on the impinging DC current, making data interpretation difficult. Hence, measurements were also performed at 40 mK and at 90 mK, where the transmission dependence on the current weakens and the excess noise agrees with equation (2)

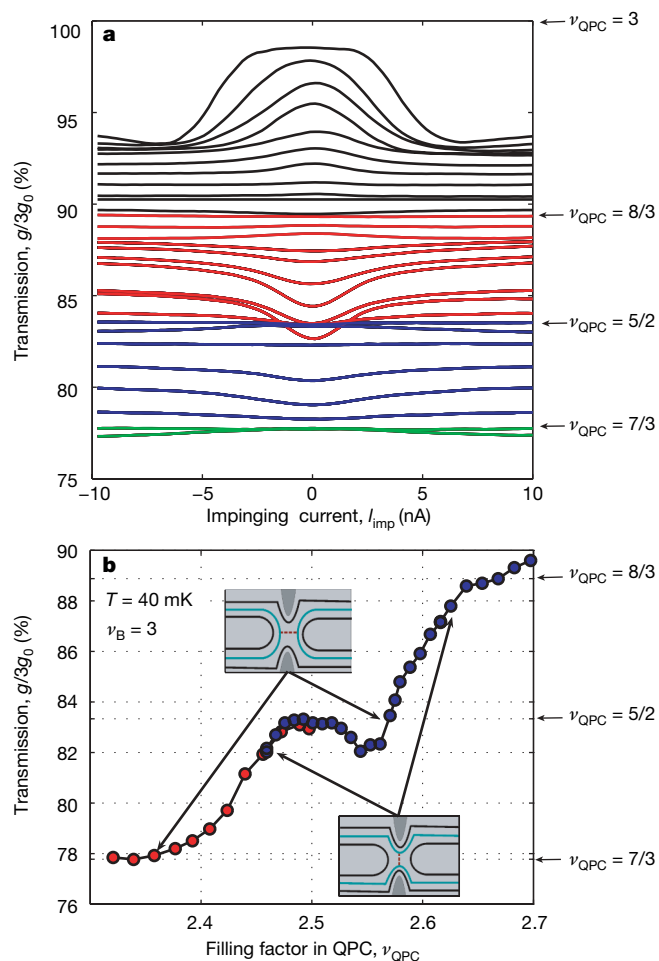


**Figure 2** | The procedure used to identify lower lying states within the QPC.

**a**, Differential transmission of the QPC as a function of impinging current at different filling factors in the QPC,  $\nu_{\text{QPC}}$ , which are adjusted by the gate voltage and the magnetic field (while staying on the  $\nu_B = 3$  plateau). Each fraction formed within the QPC is identified by a flat dependence of the conductance as function of current, surrounded by a 'mound-like' dependence for a slightly lower filling factor and a 'valley-like' dependence for a slightly higher filling factor. Three underlying states were found using this method: lines are shown black for the partitioned state, red for  $8/3$ , blue for  $5/2$ , and green for  $7/3$ . The valley crossing near  $\nu_{\text{QPC}} = 5/2$  is due to the integer quantum Hall re-entrant behaviour near that fraction. **b**, Linear transmission (at zero DC current) of the QPC as a function of  $\nu_{\text{QPC}}$ . The two colours designate two different gate voltages; at each gate voltage the filling factor was tuned with the magnetic field (on the  $\nu_B = 3$  plateau). The two insets show schematically regions of weak backscattering (under a plateau; bottom inset), and regions of strong backscattering (just above the lower lying plateau; top inset).

(see Supplementary Information for more details), suggesting an almost single particle-like behaviour (see also refs 11, 21, 22, 26). The nonlinear transmission was taken into account using two different models for the effective transmission  $t_{v_i-v_{i-1}}$ : a differential model, where for each value of the total impinging current,  $I_{\text{imp}}$ , we take  $t_{v_i-v_{i-1}} \equiv t_{\text{diff}}(I_{\text{imp}}) = \frac{g(I_{\text{imp}}) - g_{i-1}}{\Delta g_i}$ ; and an average model,  $t_{v_i-v_{i-1}} = t_{\text{aver}}(I_{\text{imp}})$ , where the transmission is obtained by an average of the differential transmissions in the current range  $0 - I_{\text{imp}}$ . Whereas in the differential model the underlying assumption is that the potential barrier in the QPC is affected by the applied voltage, in the average model we assume implicitly that the potential barrier in the QPC is independent of the applied voltage. Although each model is not accurate, they represent a lower and an upper limit of the transmission of the QPC.

Measurements of shot noise were performed in a wide range of filling factors in the QPC ( $\nu_{\text{QPC}} = 5/3 \dots 3$ ), while in the bulk the filling factor was kept at  $\nu_B = 2$ ,  $\nu_B = 5/2$  or at  $\nu_B = 3$ . The corresponding charge of the quasiparticles in state  $v_i$  is best measured at the weak backscattering limit of that state, as one expects then rare and independent backscattering events, and moreover, a weaker dependence of the effective transmission on the correct identification of the next lower lying channel,  $v_{i-1}$ . Note that although equation (2) should also be valid at small transmission, the charge of the quasiparticles may change in this limit, reflecting already the nature of the

next lower lying state,  $v_{i-1}$  (ref. 28). In our set-up, a weak and persistent reflection by the QPC, even at an applied zero gate voltage, prevented a sufficiently small backscattering coefficient being reached at  $\nu_B = 5/2$ , so we also conducted measurements at bulk filling  $\nu_B = 3$  with the QPC tuned to filling factors in the range  $\nu_{\text{QPC}} = 7/3 \dots 5/2$ , as we describe below.

### Shot noise measurements and charge determination

Conductance and shot noise measurements were conducted at different bulk filling factors and were analysed on the basis of our method of identifying the lower lying states in the QPC described above. As will be shown below, we also tested, when in question, the consequence of a different choice of the next lower lying channel (see Supplementary Information for more details).

We started with measurements of a partitioned  $5/2$  state within the QPC while the bulk filling factor was  $\nu_B = 3$ . The conductance and shot noise are plotted as function of the total impinging DC current  $I_{\text{imp}} = 3Ve^2/h$  at a temperature of 40 mK (Fig. 3). The impinging current and the differential transmission were calculated under the assumption that the lower channel is  $\nu_{\text{QPC}} = 7/3$  (see measurement results in Fig. 2), namely,  $I_{\text{imp}}(i) = V\Delta g_{5/2} = V\frac{e^2}{6h}$  and  $t_{5/2-7/3} = \frac{g(I_{\text{imp}}) - g_{7/3}}{\Delta g_{5/2}} = 0.55 - 0.72$  (as the impinging current increases). The two models for the effective transmission ( $t_{\text{diff}}$  and  $t_{\text{aver}}$ ) led to similar predictions for the expected noise, with that for charge  $e^* = e/4$  plotted in Fig. 3 (black line). Although the scattering of the data was relatively large (even after 48 h of measurement time), the agreement with  $e^* = e/4$ , excluding thus  $e^* = e/2$  (also plotted for comparison), is evident. We note that assuming a next lower lying channel  $\nu_{\text{QPC}} = 2$  does not significantly change our conclusion. In the latter case, the effective transmission varies in the range 0.86–0.90 and the analysis of the shot noise agrees with a quasiparticle charge  $e^* = e/5 - e/4$ ; this definitely excludes a charge  $e^* = e/2$  (see Supplementary Information).

In order to further study the quasiparticles' charge, we also performed measurements at bulk filling factor  $\nu_B = 5/2$  and different QPC transmissions. Measurements of the nonlinear conductance (similar to Fig. 2) were performed in order to verify the next lower lying channel. They revealed that for these parameters the next lower lying state in the QPC was  $\nu_{\text{QPC}} = 2$ . Moreover, the absence of the  $\nu_{\text{QPC}} = 7/3$  lower channel was also verified: first, by not observing a flat transmission as a function of impinging current, and second, by the absence of noise suppression when the conductance corresponded to  $\nu_{\text{QPC}} = 7/3$ . Figure 4 displays three measurements of shot noise as a function of the total impinging current  $I_{\text{imp}}$ : Fig. 4a, b, with measurements at 10 mK and at a reasonably weak backscattering; Fig. 4c, d, with measurements at 10 mK and transmission  $t_{5/2-2} \approx 0.5$ ; and Fig. 4e, f, with measurements at 40 mK and very strong backscattering. For weak backscattering (Fig. 4b), both models for the effective transmission coincide, leading to quasiparticle charge  $e^* = e/4$  (the curve for  $e^* = e/2$  is also shown for comparison). Figure 4d presents data where the reliability of equation (2) is questionable (as the transmission is intermediate, the scattering events may not be independent), and the two models for transmission clearly deviated from each other (shown in the figure). Here, the apparent charge is again close to  $e^* = e/4$  although the data fit better to a charge  $e^* \approx 0.2e$ . When the  $5/2$  channel is almost completely pinched at zero impinging current, and the transmission is highly nonlinear and changes from 2% to 20% as function of the current (Fig. 4e), again both models for the transmission provide an upper and lower limit for the shot noise, yet corresponding nicely to a quasiparticle charge  $e^* = e/4$  (Fig. 4f). This is somewhat surprising, because one might have expected that (in this strong backscattering regime, with the next lower lying channel  $\nu_{\text{QPC}} = 2$ ) the tunnelling particle would be an electron.

It is obviously desirable to measure the effective charge at different quantum Hall states in the same device in the vicinity of  $\nu_{\text{QPC}} = 5/2$ . Figure 5 summarizes some of the measurements that we did in the

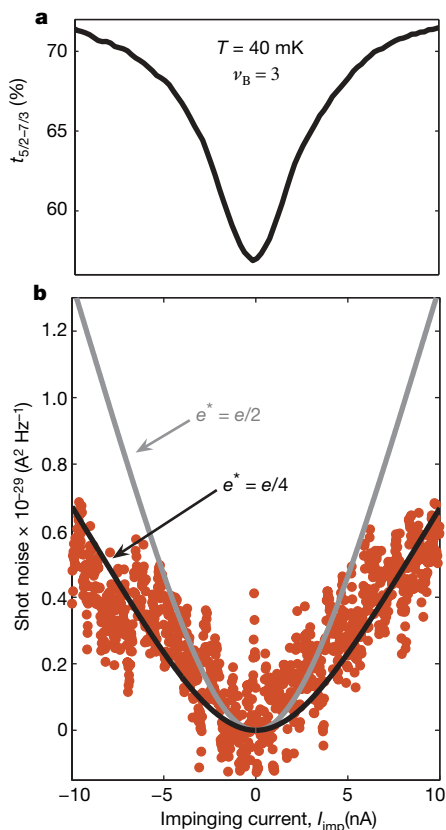


**Figure 3 | Conductance and shot noise measurements of partitioned particles at the  $5/2$  state.** **a, b**, For a filling factor in the bulk  $\nu_B = 3$  and that in the QPC tuned to weak backscattering of the  $5/2$  state, transmission **(a)** and shot noise **(b)** were measured as function of the impinging current  $I_{\text{imp}} = Vg_i$  with  $g_i = 3e^2/h$ . The effective transmission of the partitioned channel was calculated assuming that the lower state below the  $5/2$  is the  $7/3$  state (see Fig. 2). Measurement points (1,000) were taken over 40 s, as the impinging current changed from  $-10$  nA to  $10$  nA. This measurement was repeated a few hundred times, and then averaged. The amplification system, calibrated with a calibrated noise signal at 4.2 K, had a voltage gain of 2,000. In **b**, the predicted shot noise (equation (2)) for charge  $e^* = e/4$  (black line) and for  $e^* = e/2$  (grey line) is plotted on the data. The data exclude the contribution of charge  $e^* = e/2$  to the noise.

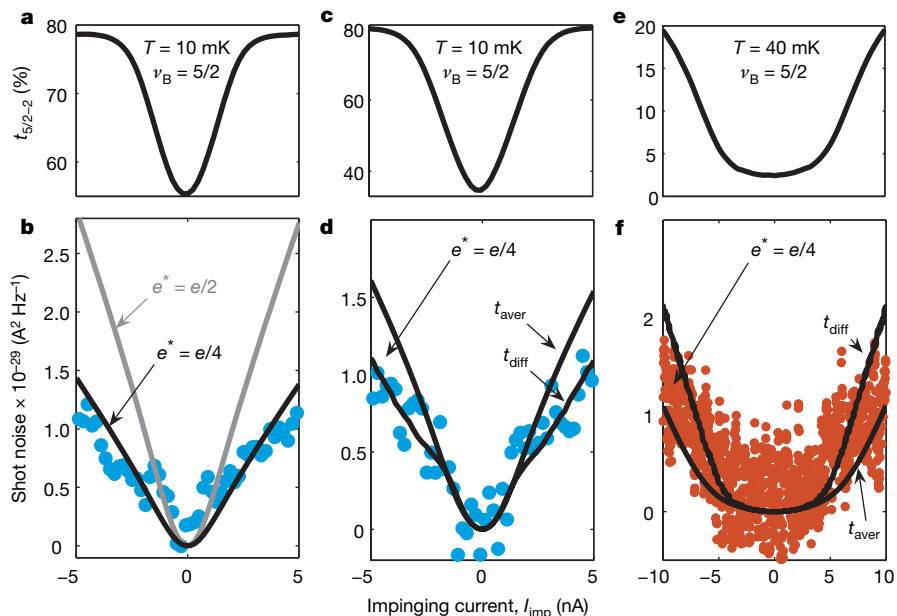


**Figure 4 | Conductance and shot noise measurements of partitioned particles at the 5/2 state, with a filling factor in the bulk of  $\nu_B = 5/2$ .** Transmission and shot noise were measured as function of the impinging current  $I_{imp} = Vg_i$ , with  $g_i = 2.5e^2/h$ . The effective transmission of the partitioned channel was calculated assuming that the lower state below the  $\nu = 5/2$  is the  $\nu = 2$  state, determined by a similar method to that described in Fig. 2. Measurements were done in a similar fashion to that described in Fig. 3, but some of the data are represented by fewer points, which were

obtained after averaging. **a, b**, Measurements at 10 mK, at weak backscattering, where both models of the transmission coincide (see text). **c, d**, Measurements at 10 mK, transmission  $\sim 0.5$ , where the two models for the transmission provide the two limits of the expected noise. **e, f**, Measurements at 40 mK, strong backscattering, where the two models for the transmission provide the two limits of the expected noise. Surprisingly, the charge remains  $e^* = e/4$ , with no evident ‘bunching’ to  $e$  when the QPC is nearly pinched.

range  $\nu_{QPC} = 5/3 \dots 3$ , identified on the two-terminal Hall conductance of the actual sample on which the measurements were made. In the top row, we show the effective transmission of the state under study with the identification of the next lower lying state, which was identified by the method shown in Fig. 2 (in some of the cases we did not plot the conductance and shot noise due to lack of space, but

present them in Supplementary Information). The panel at top left in Fig. 5 was measured at  $\nu_B = 3$ , with relatively weak backscattering induced by the QPC. The transmission drops with increasing current in a ‘mound-like’ fashion and saturates around 5 nA. The saturation at higher currents (or voltage) is typical (see, for example, ref. 26), and is accompanied by a saturation of the shot noise. It could be

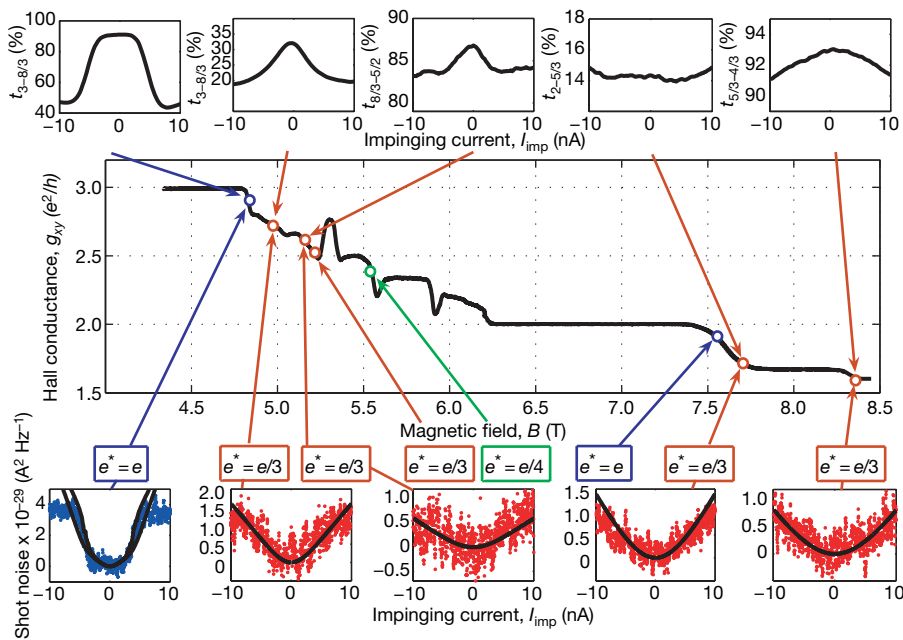


**Figure 5 | Conductance and shot noise at different filling factors in the QPC.** The main plot shows the two-terminal Hall conductance of the sample as a function of magnetic field; measurement points are indicated on this curve. For each measurement point, the top row shows the transmission as a function of impinging current, and the bottom row shows the shot noise as a function of impinging current. Measured charge is shown boxed below the

main plot. Except for the 5/2 state, measurements in the range  $\nu_{QPC} = 3 \dots 2$  were performed at  $\nu_B = 3$  and at  $T = 40$  mK, and measurements in the range  $\nu_{QPC} = 2 \dots 5/3$  were performed at  $\nu_B = 2$  and at  $T = 90$  mK. Near integer fillings (2 and 3) the measured charge was  $e$ , whereas near (above and below) the fractional fillings (8/3 and 5/3) the measured charge was  $e/3$ .

related to the deforming shape of the barrier or interactions (charging) induced by the increased current. Here, near  $\nu_{\text{QPC}} = 3$ , we observed a nice agreement with charge  $e$ , as expected (bottom left panel in Fig. 5). Pinching the QPC further, as in the second panel, the conductance approaches the one corresponding to  $\nu_{\text{QPC}} = 8/3$ , and the charge fractionalizes with a clear quasiparticle charge  $e^* = e/3$  (second panel, bottom row). A very similar behaviour is observed when the filling factor in the QPC is slightly lower than  $\nu_{\text{QPC}} = 2$  (measured at  $\nu_B = 2$  and at a temperature of 90 mK), agreeing with a charge  $e$ , as expected. This charge fractionalized to  $e^* = e/3$  as the filling factor lowered to just above  $\nu_{\text{QPC}} = 5/3$ . Such fractionalization of the charge as the effective barrier for electrons increases was surprising at first. We attribute it to the formation of a FQHE region of  $\nu_{\text{QPC}} = 5/3$  within the QPC, separating the two regions on both sides of the QPC. Then, the observed fractional charge may be viewed as the charge of the quasi-holes with charge  $e^* = e/3$  tunnelling across the  $\nu_{\text{QPC}} = 5/3$  region. When the filling factor in the QPC drops further to slightly below  $\nu = 5/3$ , and similarly also below  $\nu = 8/3$ , we also measured  $e^* = e/3$ , as was expected<sup>11</sup> (see panels in Fig. 5).

## Discussion

We have presented direct evidence of a quasiparticle charge of  $e^* = e/4$  at an even denominator fractional filling of  $5/2$  in the second Landau level of the quantum Hall effect. The affirmation of the predicted charge of the quasiparticles is a strong indication that the  $\nu = 5/2$  is a paired state, where pairs of composite fermions condense into a gapped state. It is consistent with the Moore–Read<sup>4</sup> theory, and indicates that if this theory is indeed correct, the quasiparticles that tunnel across a point contact are non-abelian quasiparticles with charge  $e/4$ . Our experiment does not probe the non-abelian statistics: in order to do this, a direct measurement (say, via interference<sup>7,13–16,29</sup>) should be conducted. Finally, we also measured the charge of quasiparticles in adjacent filling factors.

## METHODS SUMMARY

**The 2DEG and the sample.** Our structure consisted of a 29-nm-wide GaAs- $\text{Al}_{0.25}\text{Ga}_{0.75}\text{As}$  quantum well, doped on both sides with Si ‘delta-doping’ (a deposited fraction of a Si monolayer). The two ‘delta-doping’ layers were placed in narrow quantum wells, being part of a short period superlattice, separated from the 2DEG by an undoped  $\text{Al}_{0.25}\text{Ga}_{0.75}\text{As}$  layer with thickness 80 nm. The 2DEG was located 160 nm below the surface, with the AlAs mole fraction rising to 35% near the surface.

The sample was patterned by optical lithography and electron beam lithography. Measurements were done on an unilluminated sample. The conductance of the QPC was found to be irreproducible as a function of gate voltage, and tended to vary as function of time after the gate voltage was changed.

Note that the 2DEG mobility and the quantum scattering time were found to be poor indicators for the ‘quality of FQHE features’. Some lower-mobility samples (around  $15 \times 10^6 \text{ cm}^2 \text{ V}^{-1} \text{ s}^{-1}$ ) showed nice fractional states, while higher-mobility samples (as high as  $36 \times 10^6 \text{ cm}^2 \text{ V}^{-1} \text{ s}^{-1}$ ) sometimes showed poorer behaviour.

**Measuring shot noise.** Using a multi-terminal configuration ensured that the sample conductance in a quantum Hall plateau was at a constant  $\nu e^2/h$  value and independent of the QPC transmission. To avoid the large  $1/f$  noise at low frequencies, a resonant circuit was connected between the drain (D) and ground, made of a copper coil ( $L$ ) and a capacitor ( $C$ ), tuned to a resonance frequency of 910 kHz. This was followed by a home-made preamplifier cooled to 4.2 K, a room temperature amplifier (NF SA-220F5), and a spectrum analyser (bandwidth 30 kHz or 100 kHz).

Comparing the expected spectral density of the voltage noise  $S_v^v$  at  $\nu = 1/3$  and at  $\nu = 5/2$ , we find  $S_{1/3}^v/S_{5/2}^v = 50$ . As the signal (the shot noise) to noise (the uncorrelated system noise) ratio is proportional to  $(\Delta f \times \tau)^{-1/2}$ , with  $\Delta f$  the bandwidth, an unreasonable 2,500 times longer measurement time  $\tau$  is required for the same signal to noise ratio. Hence, a larger voltage was applied ( $V = 10$ – $100 \mu\text{V}$ , with the associated energy  $e^*V$  being some 10–100 times larger than the thermal energy  $k_B T$ ); combined with a wider bandwidth of the  $LC$  circuit at the  $\nu = 5/2$  state (due to the higher conductance), it enabled a more reasonable measurement time.

**Full Methods** and any associated references are available in the online version of the paper at [www.nature.com/nature](http://www.nature.com/nature).

Received 9 November 2007; accepted 14 February 2008.

1. Tsui, D. C., Stormer, H. L. & Gossard, A. C. Two-dimensional magnetotransport in the extreme quantum limit. *Phys. Rev. Lett.* **48**, 1559–1562 (1982).
2. Prange, R. E. & Girvin, S. M. (eds) *The Quantum Hall Effect* (Springer, New York, 1987).
3. Willett, R. et al. Observation of an even-denominator quantum number in the fractional quantum Hall effect. *Phys. Rev. Lett.* **59**, 1776–1779 (1987).
4. Moore, G. & Read, N. Nonabelions in the fractional quantum Hall effect. *Nucl. Phys. B* **360**, 362–396 (1991).
5. Read, N. Paired fractional quantum Hall states and the  $\nu=5/2$  puzzle. Preprint at (<http://arxiv.org/abs/cond-mat/0011338>) (2000).
6. Kitaev, A. Fault tolerant quantum computation by anyons. *Ann. Phys. (NY)* **303**, 2–30 (2003).
7. Das Sarma, S., Freedman, M., Nayak, C., Simon, S. & Stern, A. Non-abelian anyons and topological quantum computation. Preprint at (<http://arxiv.org/abs/0707.1889>) (2007).
8. Das Sarma, S., Freedman, M. & Nayak, C. Topologically protected qubits from a possible non-abelian fractional quantum Hall state. *Phys. Rev. Lett.* **94**, 166802 (2005).
9. Read, N. & Green, D. Paired states of fermions in two dimensions with breaking of parity and time-reversal symmetries and the fractional quantum Hall effect. *Phys. Rev. B* **61**, 10267–10297 (2000).
10. Morf, R. H. Transition from quantum Hall to compressible states in the second Landau level: New light on the  $5/2$  enigma. *Phys. Rev. Lett.* **80**, 1505–1508 (1998).
11. de Picciotto, R. et al. Direct observation of a fractional charge. *Nature* **389**, 162–164 (1997).
12. Saminadayar, L., Glattli, D. C., Jin, Y. & Etienne, B. Observation of the  $e/3$  fractionally charged Laughlin quasiparticles. *Phys. Rev. Lett.* **79**, 2526–2529 (1997).
13. Stern, A. & Halperin, B. I. Proposed experiments to probe the non-abelian  $\nu=5/2$  quantum Hall state. *Phys. Rev. Lett.* **96**, 016802 (2006).
14. Fradkin, E. et al. A Chern-Simons effective field theory for the Pfaffian quantum Hall state. *Nucl. Phys. B* **516**, 704–718 (1998).
15. Bonderson, P., Kitaev, A. & Shtengel, K. Detecting non-abelian statistics in the  $\nu=5/2$  fractional quantum Hall state. *Phys. Rev. Lett.* **96**, 016803 (2006).
16. Feldman, D. E., Gefen, Y., Kitaev, A., Law, K. T. & Stern, A. Shot noise in anyonic Mach-Zehnder interferometer. *Phys. Rev. B* **76**, 085333 (2007).
17. Toke, C. & Jain, J. K. Understanding the  $5/2$  fractional quantum Hall effect without the Pfaffian wave function. *Phys. Rev. Lett.* **96**, 246805 (2006).
18. Pan, W. et al. The other even-denominator fractions. *Physica E* **9**, 9–16 (2001).
19. Miller, J. B. et al. Fractional quantum Hall effect in a quantum point contact at filling fraction  $5/2$ . *Nature Phys.* **3**, 561–565 (2007).
20. Chung, Y. C., Heiblum, M. & Umansky, V. Scattering of bunched fractionally charged quasiparticles. *Phys. Rev. Lett.* **91**, 216804 (2003).
21. Griffiths, T. G., Comforti, E., Heiblum, M., Stern, A. & Umansky, V. Evolution of the quasiparticle charge in the fractional quantum Hall regime. *Phys. Rev. Lett.* **85**, 3918–3921 (2000).
22. Reznikov, M. et al. Observation of quasiparticles with one-fifth of an electron’s charge. *Nature* **389**, 238–241 (1999).
23. Lesovik, G. B. Excess quantum shot noise in 2D ballistic point contacts. *JETP Lett.* **49**, 592–594 (1989).
24. Bena, C. & Nayak, C. Effects of non-Abelian statistics on two-terminal shot noise in a quantum Hall liquid in the Pfaffian state. *Phys. Rev. B* **73**, 155335 (2006).
25. Martin, T. & Landauer, R. Wave packet approach to noise in multi-channel mesoscopic systems. *Phys. Rev. B* **45**, 1742–1755 (1992).
26. Chung, Y. C. et al. Anomalous chiral Luttinger liquid behavior of diluted fractionally charged quasiparticles. *Phys. Rev. B* **67**, 201104 (2003).
27. Roddaro, S., Pellegrini, V. & Beltram, F. Particle-hole Luttinger liquids in a quantum Hall circuit. *Phys. Rev. Lett.* **95**, 156804 (2005).
28. Kane, C. L. & Fisher, M. P. A. Nonequilibrium noise and fractional charge in the quantum Hall effect. *Phys. Rev. Lett.* **72**, 724–727 (1994).
29. Stevn, A. Anyons and the quantum Hall effect—A pedagogical review. *Ann. Phys.* **1**, 204–249 (2008).

**Supplementary Information** is linked to the online version of the paper at [www.nature.com/nature](http://www.nature.com/nature).

**Acknowledgements** We thank A. Ra’anan for laying the foundations for these experiments; A. Schreier, I. Neder, N. Ofek, Y. Gross, E. Grosfeld, Y. Gefen, B. I. Halperin, Y. Levinson, B. Rosenow and S. Das Sarma for their suggestions and assistance; J. Miller and C. Marcus for sharing with us their experience of the fabrication process; and L. Pfeiffer for providing us with a sample for initial experimentation. M.H. acknowledges partial support from the Israeli Science Foundation (ISF), the German Israeli Foundation (GIF), and the Minerva Foundation. A.S. acknowledges support from the US-Israel Bi-national Science Foundation, the Minerva foundation, and the ISF.

**Author Information** Reprints and permissions information is available at [www.nature.com/reprints](http://www.nature.com/reprints). Correspondence and requests for materials should be addressed to M.D. ([merav.dolev@weizmann.ac.il](mailto:merav.dolev@weizmann.ac.il)).

## METHODS

**The 2DEG.** The enabling ingredient for the experiment is the quality of the 2DEG. Only extremely high-mobility structures showed the fragile even denominator  $5/2$  fraction. The electron density of our 2DEG was  $\sim 3.2 \times 10^{11} \text{ cm}^{-2}$ , with a low-temperature mobility of  $30.5 \times 10^6 \text{ cm}^2 \text{ V}^{-1} \text{ s}^{-1}$ , measured in the dark. The quantum scattering time of the electrons was estimated from Shubnikov de Haas oscillations to be around 12 ps. Our heterostructure consisted of a 29-nm-wide GaAs- $\text{Al}_{0.25}\text{Ga}_{0.75}\text{As}$  quantum well containing the 2DEG, doped on both sides with Si 'delta-doping', which serve as donors. The two 'delta-doping' layers were also placed in narrow quantum wells, being part of a short period superlattice, separated from the 2DEG by an undoped  $\text{Al}_{0.25}\text{Ga}_{0.75}\text{As}$  layer (spacer) with thickness 80 nm. Uniform doping, some 60 nm below the surface, compensated the surface states and thus terminated the depletion layer. The 2DEG was located 160 nm below the surface, with the AlAs mole fraction rising from 25% at the uniform doping to 35% near the surface. A thin GaAs cap terminated the structure in order to prevent oxidation and facilitate better ohmic contacts.

**The mobility of the 2DEG.** Note that the mobility of 2DEG and the quantum scattering time were found to be rather poor indicators for the 'quality of FQHE features'. Indeed, high-mobility 2DEGs are needed to observe the fragile fractional states, however, in this high range some lower-mobility samples (around  $15 \times 10^6 \text{ cm}^2 \text{ V}^{-1} \text{ s}^{-1}$ ) showed nice fractional states while higher-mobility samples (as high as  $36 \times 10^6 \text{ cm}^2 \text{ V}^{-1} \text{ s}^{-1}$ ) showed sometimes poorer behaviour. This behaviour is poorly understood, however, as the mobility and quantum times represent only the second order correlator of the potential fluctuations, and it is likely that higher order correlators (namely, the detailed shape of the potential landscape) are responsible for the localization in high magnetic field.

**The sample.** The samples were patterned in a shape of a Hall bar, with a single QPC in its centre and multiple ohmic contacts. The QPC partitioned the incoming current by bringing the forward propagating edge channel, with a chemical potential determined by the applied voltage  $V$ , into close proximity with the backward propagating edge channel returning from the grounded contact, hence inducing backscattering, partitioning and shot noise. Two contacts, 1 and 2, were grounded directly to the cold finger ('cold grounds'), which was attached directly to the mixing chamber, in order to cool the electrons to  $\sim 10$  mK. When needed, a heater was used to heat the mixing chamber, and hence the sample, above base temperature. The sample was patterned by optical lithography and electron beam lithography. Metallic gates were formed by deposition of 15 nm of PdAu and 15 nm of Au. Measurements were done on unilluminated samples. The conductance of the QPC was found to be irreproducible as a function of the gate voltage, and tended to vary as function of time after the gate voltage was changed. Hence, the desired conductance was achieved by tuning the gate voltage and the magnetic field along the quantum Hall plateau.

**Measuring shot noise.** A DC current  $I_{\text{imp}}$  was driven from the source contact (S), with the QPC partitioning it to the transmitted and backscattered currents. To avoid the large  $1/f$  noise at low frequencies, a resonant circuit was connected between the drain (D) and ground, made of a copper coil ( $L$ ) and a capacitor ( $C$ , formed mostly by the capacitance of the coaxial cable), tuned to a resonance frequency of 910 kHz. This was followed by a home-made preamplifier cooled to 4.2 K, a room temperature amplifier (NF SA-220F5), and a spectrum analyser (bandwidth 30 kHz or 100 kHz). The multi-terminal configuration of the sample ensured a constant input resistance to the preamplifier when the quantum Hall effect was tuned to a conductance plateau, independent of the transmission of the QPC (as long as the longitudinal resistance was zero, the resistance between terminals D and 2 was always the Hall resistance). This allowed the 'resistance dependent' noise components, namely, the 'current noise' of the preamplifier (backward injected current by the preamplifier into the sample) and the thermal noise of the sample (together being some 50 times larger than the desired shot noise signal), to be subtracted from the measured total signal (their summed value was measured by setting the impinging current to zero).

Comparing the expected spectral density of the voltage noise  $S^v$  at  $\nu = 1/3$  and at  $\nu = 5/2$ , we find  $S^v_{1/3}/S^v_{5/2} = 50$ . As the signal-to-noise ratio (the shot noise to the uncorrelated system noise ratio) is proportional to  $(\Delta f \times \tau)^{-1/2}$ , with  $\Delta f$  the bandwidth and  $\tau$  the measurement time, an unreasonable measurement time (2,500 times longer) was required for the same signal to noise ratio. Hence, a larger voltage (and current) was applied (10–100  $\mu\text{V}$ , being some 10–100 times larger than the electron temperature), which combined with a wider bandwidth of the  $LC$  circuit at the  $\nu = 5/2$  state (due to the relatively high conductance) enabled a more reasonable measurement time.